

## Mineralogy, Micro-fabric and the Behavior of the Completely Decomposed Granite Soils

Elsayed Elkamhawy <sup>a, b</sup>, Bo Zhou <sup>a</sup>, Huabin Wang <sup>a\*</sup>

<sup>a</sup> School of Civil Engineering and Mechanics, Huazhong University of Science and Technology, Wuhan, Post code 430074, P.R. China.

<sup>b</sup> Faculty of Engineering, Zagazig University, Zagazig, Post code 44519, Egypt.

Received 16 September 2019; Accepted 20 November 2019

### Abstract

The main objective of this study is to investigate the impact of the micro-fabric and soil mineralogy on the overall macro-behavior of the completely decomposed granite soil through a set of drained and undrained triaxial shearing and isotropic compression tests on a medium-coarse grading completely decomposed granite soil. The mineral composition of the soil was a substantial factor governing the compressive behavior. The soil compressibility increased significantly in the case of existence crushable and weak minerals within the soil minerals like fragile feldspar, as well as the high content of fines, especially the plastic fines. The scanning electron microscopic photos indicated that the micro-fabric of the soil had a paramount impact on the compressive behavior. The mechanism of the volumetric change depended on the stress levels, the soil mineral composition and the grain morphology. In the low consolidated stress levels, the soils' grains rearrangement was the prevailing mechanism of the volumetric change, particularly with the absence of weak and crushable minerals. On the other hand, at the high consolidated stress levels, particles' crushing was the prevailing mechanism in the volumetric change. Both the mechanisms of volume change could occur simultaneously at the low stress levels in the case of presence crushable minerals in addition to micro-cracks in the soil grains. The soil showed an isotropic response after 250 kPa, as this stress level erased the induced anisotropy from the moist tamping preparation method. Under the drained shearing conditions, the soil showed a contractive response, while during the undrained shearing conditions, the soil exhibited both the contractive and dilative responses with phase transformation points. The studied soil showed a unique critical state line, irrespective of the drainage conditions and initial states, the critical state line was parallel to the isotropic compression line in the void ratio–effective stress space. In the deviator–effective mean stresses space, the studied soil approached a unique CSL with a critical stress ratio equal 1.5, corresponding to critical friction angle of 36.8°.

**Keywords:** Completely Decomposed Granite; Soil Mineralogy; Micro-fabric.

### 1. Introduction

Because of the abundance of the completely decomposed granite (CDG) soil in many countries around the world, it is vastly utilized in engineering practices for example: back-fill materials for retaining walls, construction of earth dams, embankments of waterways, and roads. Behavior of residual soils is completely different from sedimentary soils. Residual soils such as granitic saprolite soils originated from the chemical and physical weathering processes of granite rock, thus the mineralogy and micro-fabric of the parent rock are considered substantial factors governing the resulted soils behavior [1]. Residual soils are generally well-graded and include a broad domain of grain size distributions [2]. Many studies have shown that the grading of granitic saprolite soil depends on the environmental circumstances of the

\* Corresponding author: [huabin@mail.hust.edu.cn](mailto:huabin@mail.hust.edu.cn)

 <http://dx.doi.org/10.28991/cej-2019-03091447>



© 2019 by the authors. Licensee C.E.J., Tehran, Iran. This article is an open access article distributed under the terms and conditions of the Creative Commons Attribution (CC-BY) license (<http://creativecommons.org/licenses/by/4.0/>).

weathering process, mineralogy and micro-fabric of the parent rock; in which the soil grading curve shifts towards the fine domain as the weathering grade increases [3-6].

On account of shortage and insufficient data available about mineral composition of soils in addition to grains morphology, researchers have concluded that grading is considered the dominant factor in the compressive behavior of saprolitic soils [2, 7]. Ham, Nakata [8] found that content of gravel had a significant impact on the compression characteristics of CDG soils. Ham, Nakata [9] have shown that the compressibility of CDG soil is robustly affected by the strength of single particle. Studies conducted on CDG soils have shown that the uniqueness of isotropic compression lines (ICLs) is a general feature of such these kinds of soil [10-12]. However, nonuniqueness of ICLs was observed by Wang and Yan [13], as the ICLs were nearly parallel; such behavior is termed “transitional behavior”, which could be attributed to the soil fabric. Wang and Yan [13] investigated undisturbed soil, while, re-compacted samples have been reported by Yan and Li [12], Ng, Fung [11], and Lee and Coop [10]. Therefore, the impact of the parent rock fabric is clearly pronounced in the intact soil behavior. The non-uniqueness of ICLs was also reported by Elkamhawy, Zhou [14] in the reconstituted CDG soil by increasing sand contents, thus the induced fabric by increasing sand content withstood during the isotropic compression path.

Unique critical state lines (CSLs) were also found in the deviator and effective mean stresses  $q$ - $p'$  space and in the  $e$ - $\log p'$  space, regardless of the drainage conditions and initial states. Although the reconstituted CDG soil and intact soil samples reported by Elkamhawy, Zhou [14] and Wang and Yan [13], respectively exhibited nonuniqueness of the ICLs, unique CSLs were also found in the  $e$ - $\log p'$  space. This could be explained as follows; whatever the fabric triggered from the isotropic compression stage, it was not sturdy enough to persist during shearing, and it was completely destroyed during large strain-shearing path, leading eventually to unique CSL.

To meet the rapid development in china, granitic saprolites are extensively used in many engineering applications. Because of the shortage in studies that dealt with these soils, the behavior is not well understood and many engineering problems occurred, in addition to the fact that the weathered rocks get involved in various modes of landslides [15, 16] leading to loss of lives and property. Thus there is urgent need for further studies to understand the mechanics of this kind of soil. Therefore, the main objectives of the current paper are providing well understanding of the CDG soil behavior and illuminating the influences of the micro-fabric and mineralogy on the mechanical characteristics via a set of drained and undrained triaxial compression shearing and isotropic compression tests performed on medium-coarse CDG soil originated from the weathering of the biotite granite rock. The scanning electron microscopic photos (SEM) and X-ray diffraction analysis (XRD) have been employed to interpret the experimental results. The presented results will be more helpful for developing an advanced constitutive model for the saturated remolded CDG soils.

## 2. Research Methodology and Material Characteristics

This section provides the research methodology as indicated in Figure 1. The studied CDG soil in this paper was brought from Gaoliang city, Guangdong province, southeast China. Preliminary tests such as soil grading, specific gravity, Atterberg limits, maximum dry density, X-ray diffraction analysis, and scanning electron microscopic tests were then implemented on the studied CDG soil. After that the triaxial samples were prepared using the moist tamping technique. The soil samples were then installed in the triaxial device for saturation, consolidation, and shearing tests. The following sections indicate in detail the soil characteristics and the testing program step by step.

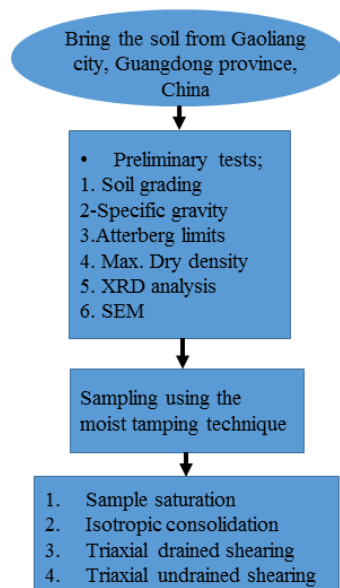


Figure 1. The flow chart of the research methodology

## 2.1. Physical Characteristics

Based on the classification system of the Geotechnical Engineering Office [17], the studied soil was completely decomposed granite (i.e., grade V). Grading curve of the CDG soil is shown in Figure 2, in addition to other reported data. It can be clearly seen that the soil is well-graded such as other CDG soils in South Korea [10] and Hong Kong [11, 12]. It can be also concluded that the environmental circumstances of the weathering process of the studied soil and the soil in Hong Kong were close, as the soils have almost close grading. The soil is classified as low plasticity clayey sand (SC-CL) based on the unified soil classification system (USCS). The maximum dry density was 1810 kg/m<sup>3</sup> at the optimum water content 15.2%. The soil specific gravity was 2.58. Plastic and liquid limits have been obtained from the fall cone test on the particles passed from No. 40 sieve (425  $\mu$ m) that were 24.65% and 39.85%, respectively.

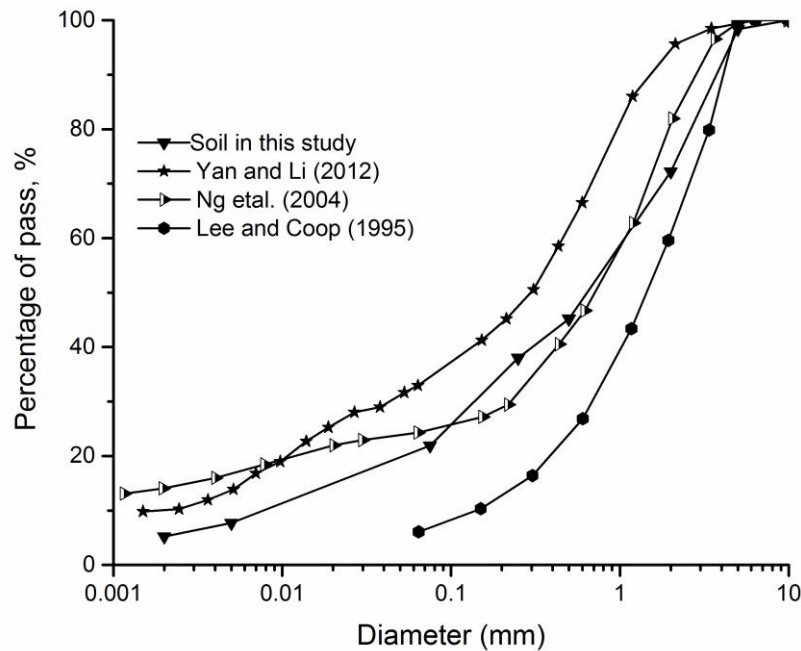


Figure 2. Soil grading

## 2.2. Mineralogical Features

By visual inspection, the CDG soil was yellowish brown with black and white spots, the geological map indicates that the parent granite rock of the CDG soil is biotite granite, as illustrated in Figure 3. In the soil site, there are no core stones, meaning that the parent biotite rock decomposed totally [18].

The X-ray diffractometer (XRD) analysis was conducted on the CDG soil samples, the XRD results were compared to the corresponding spectra for the bulk specimens of CDG. The XRD analysis showed that the soil minerals included quartz, sodium and potassium feldspar, calcite, dolomite, and clay in the form of illite and kaolinite minerals. Presence of kaolinite mineral shows well-drained conditions during the chemical weathering process. The small amounts of illite group can be attributed to the limited amounts of cations removed in a stagnant state at the slope bottom [4]. Table 1 gives the statistical analysis for the composition of the soil minerals. Quartz was found to be the most abundant mineral; this could be explained by the fact that it is inert to the chemical weathering and is considered the most stable mineral. The inert and stable minerals can be arranged starting with quartz followed by muscovite then alkali feldspar and finally plagioclase feldspar, which is considered the most mineral prone to the chemical weathering, forming finally clay minerals [19, 20]. Accordingly, the content of potassium feldspar was higher than sodium feldspar.

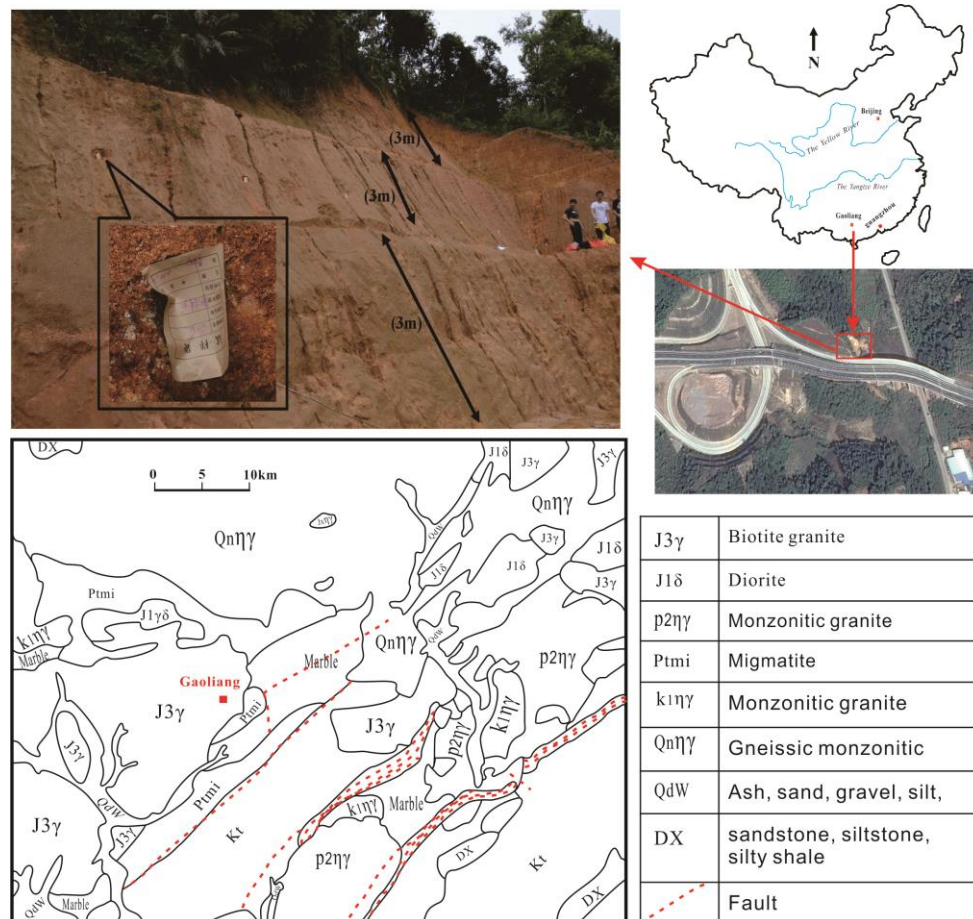


Figure 3. The soil site and geological map

Table 1. Minerals composition of the CDG soil

Mineral	Mean	Minimum	Maximum	Range
Illite	8.4	5	13	8
Kaolinite	15.8	3	22	19
Quartz	46.3	26	62	36
Potassium feldspar	27.9	19	52	33
Sodium feldspar	1	9	9	0
Dolomite	0.5	1	1	0
Calcite	0.1	1	1	0

### 2.3. Test Program and Samples Preparation

The drained and undrained triaxial shearing and isotropic compression tests were performed with an automated triaxial stress path test apparatus produced in the UK by Global Digital Systems Ltd. (GDS). The device is dependent on the classic Bishop and Wesley stress path triaxial cell, so that control directly in stresses on the soil specimen. The GDS triaxial device was provided with axial displacement controller, back and cell pressure controllers as well as a linear variable displacement transducer (LVDT) for the axial strain measurement. The GDS device permits the water drainage from the upper platen, the volume changes of the soil samples were measured through the back-pressure controller, and the pore water pressure is measured from the lower platen.

The soil sample was prepared by the moist tamping technique, as the soil was firstly oven dried and to avoid using large samples, the soil sieved through a No. 4 sieve. The sieved soil was then remixed with water at the optimum water content. After that the soil was compacted inside a split mold in three layers, with scratching between the neighboring surface layers for decreasing layering effect. By controlling the applied compaction effort and the soil weight in each layer, different initial densities were obtained. The split mold was disassembled after compaction; the soil sample was then encased by the rubber membrane. It is worth to note that the sample can stand freely after the split mold was detached and before encapsulation with the rubber membrane due to the induced suction forces, as the soil sample is partially saturated. The sample was then immersed in a tank of water under a vacuum pressure of 0.1 MPa for 24 h to increase the degree of saturation. After the preliminary saturation and prior to install sample in the GDS device, the

sample dimensions were then measured using a Vernier caliper with 0.01 mm resolution, as the diameter was measured in top, bottom and middle of the sample and taken the average value, the sample height was also measured in three positions with an angle 120° and taken the average value. The soil specimen was then combined in the triaxial apparatus with assembling all required connections. To preserve a fixed effective mean stress during the saturation process, the cell and back pressures were then increased together. To check the saturation degree, the saturation check was implemented by measuring the B-value proposed by Skempton [21], which was 0.97 for all soil samples.

During the isotropic compression test, the rates of loading and unloading were 15 kPa/h and 30 kPa/h, respectively. The induced excess pore water pressure with using these rates was not remarkable. The triaxial compression shearing test was carried out through a strain-controlled mode. A 0.02%/min and 0.05%/min axial strain rates were employed for the drained and undrained shearing, respectively, derived from Head [22]. Tables 2~4 summarize the details of the isotropic compression and the triaxial compression shearing tests. Verdugo and Ishihara [23] discussed two methods to determine the void ratio of soil samples, in this study void ratio was measured using the second method via the back calculation of the final void ratio and the volumetric change with the assumption that the soil samples are totally saturated.

**Table 2. Testing conditions for the isotropic compression tests**

Test ID	Compaction ratio	Loading path, P' kPa	Initial void ratio	Final void ratio	Slope of ICL( $\xi$ )
ISO-85	85%	20-700	0.6500	0.4760	0.06
ISO-87.5	87.5%	20-250-150-450	0.6182	0.5045	
ISO-90	90%	20-200-50-600	0.6011	0.5124	

Note: ISO means isotropic compression and the numbers refer to the compaction ratio

**Table 3. Testing conditions for the drained triaxial shearing tests**

Test type	Compaction ratio, %	Consolidated stress P'(kPa)	Void ratio before shearing	Final void ratio
Drained shearing (CD)	85.65	100	0.5740	0.5074
	85.40	200	0.5540	0.4721
	85.42	300	0.5263	0.4488
	87.68	400	0.5017	0.4318

**Table 4. Testing conditions for the triaxial undrained compression shearing tests**

Test type	Compaction ratio, %	Consolidated stress P'(kPa)	Final void ratio
Undrained shearing (CU)	88.45	100	0.5662
	85.39	200	0.5354
	87.04	300	0.5191
	86.68	400	0.4958

### 3. Isotropic Compression

Isotropic compression response of the CDG soil is depicted in Figure 4. Irrespective of the initial void ratios, the ICLs combined in a unique compression line representing the soils' state boundary surface. The unique ICL showed that the induced fabrics from the different compaction efforts were not strong enough and totally destroyed during the isotropic compression path and reached eventually a unique fabric at the end of the consolidation path. Comparing the studied soil with other reported CDG soils in Hong Kong [11, 12]. The studied soil showed low compressibility, where the gradient of the ICL ( $\xi$ ) was 0.06, which was significantly lower than those in the CDG studied by Yan and Li [12], as  $\xi$  was 0.091. This can be illustrated from the grading curves, as the studied CDG soil was much coarser with less fines content. Although the CDG soil studied by Ng, Fung [11] almost has the identical coarse content with the studied soil, the slope of the ICL was high and  $\xi$  was 0.13, this can be attributed to the high fines content, in particular the plastic fines and presence of crushable feldspar.

The low compressibility of the CDG soil can be not only imputed to soil grading, but also to the soil mineralogy and micro-fabric. Although the grading of the CDG soil in South Korea reported by Lee and Coop [10] was coarser than the studied soil, the compressibility was higher than that in the studied soil, as  $\xi$  was 0.087. This can be explained by the soil mineralogy, micro-fabric and the stress levels. The minerals composition of the CDG soil in South Korea were feldspar 50%, quartz 33% with limited amounts of kaolinite 6%, mica 9% and 2% smectite. While, the minerals of the studied CDG soil were 46.3% quartz, 28.9% feldspar, 15.8% kaolinite, and 8.4% illite with small amounts of calcite 0.1% and dolomite 0.5%. It can be clearly seen that the dominant mineral in the studied CDG soil was quartz, whereas feldspar was the dominant one for the CDG soil in South Korea. Lee and Coop [10] studied the soil under stress levels



higher than those employed in this study, presence of mica also has a paramount influence on the compressibility of the soil even if exist by a limited portion [24]. Because of the presence of the crushable feldspar and the micro-cracks in the soils' grains as well grains morphology [25], the compressibility of the CDG soil in Hong Kong was higher than that in the studied soil. A scanning electron microscopic-photo illustrated in Figure 5 indicates the micro-fabric of the CDG soil. Clay minerals not only filled feldspar fissures and pores, but also were on feldspar surface; this means that clay minerals acted as a pillow for the larger-sized minerals, thus the compressibility of the CDG soil decreased substantially.

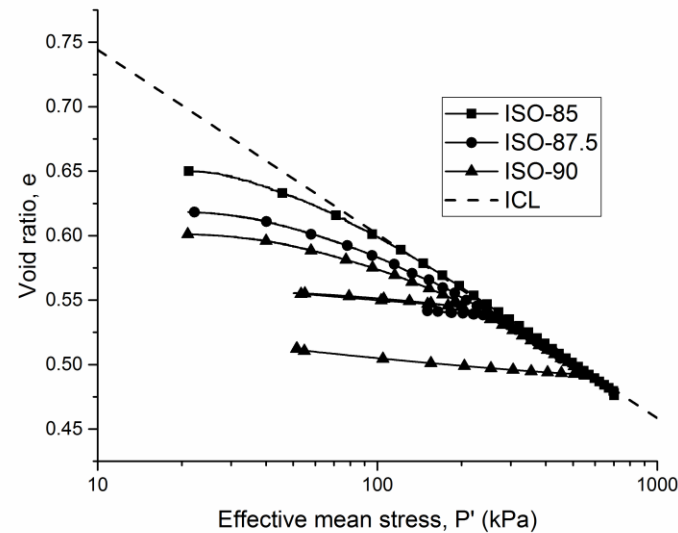


Figure 4. Isotropic compression response

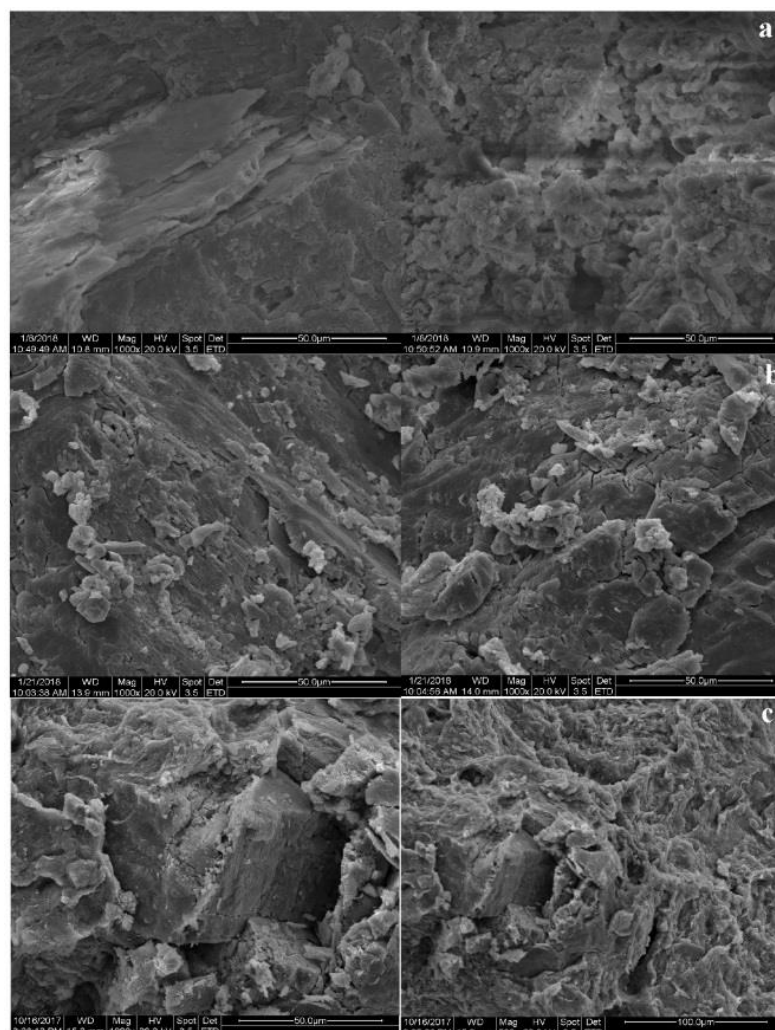


Figure 5. Scanning electron microscopic-photo a) clay minerals in feldspar fissures, b) clay minerals on feldspar surface, and c) clay minerals filling pores

#### 4. Volumetric Change

The soil specimens deformation was carefully examined during the isotropic compression and unloading stages. Figure 6 indicates the response of the soil samples, radial and axial strains were then plotted versus mean effective stresses. The soil response was represented by a 90% relative compaction. The soil exhibited an isotropic response during both the compression and relief paths. The volume change during unloading path was inconsiderable, thus volumetric change was unrecoverable. The axial strain was lower than the radial strain, which can be illustrated via the moist tamping preparation technique. When the soil specimen is compacted in a specified direction, it becomes stiffer than other direction. Therefore, the contractive behavior becomes too low in this direction, while the response becomes more contractive and softer when the soil specimen is loaded in the lateral direction [26]. These observations match closely with other CDG soils reported by Yan and Li [12] and Wang and Yan [13]. A 250 kPa effective mean stress was sufficient to erase the induced anisotropy from the compaction during the moist tamping method, in which both the axial and radial strain curves were quite parallel. Figure 7 also confirmed the isotropic response of the CDG soil, as after erasing the induced anisotropy from the preparation method, as the slope of the relation of axial and radial strains was nearly 1:1. Since the dominant mineral was quartz and the stress levels employed in this research were not high and the smaller-sized grains provide a cushion for the large-sized grains, so particles rearrangement could be the prevailing mechanism of volume change and particles crushing possibly has a limited participation.

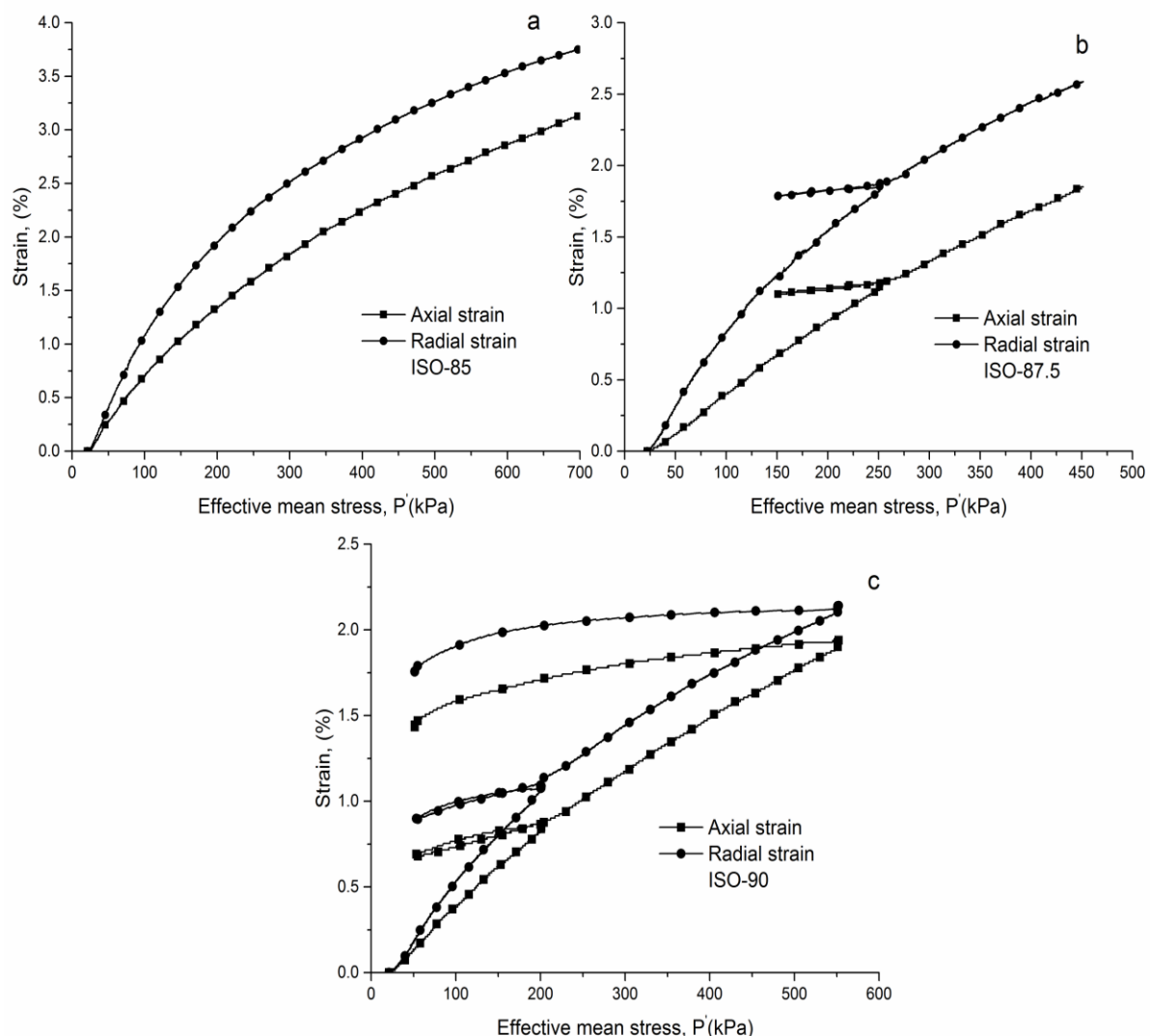


Figure 6. Variations of axial and radial strains with mean effective stresses a) compaction ratio 85%, b) compaction ratio 87.5%, and c) compaction ratio 90%

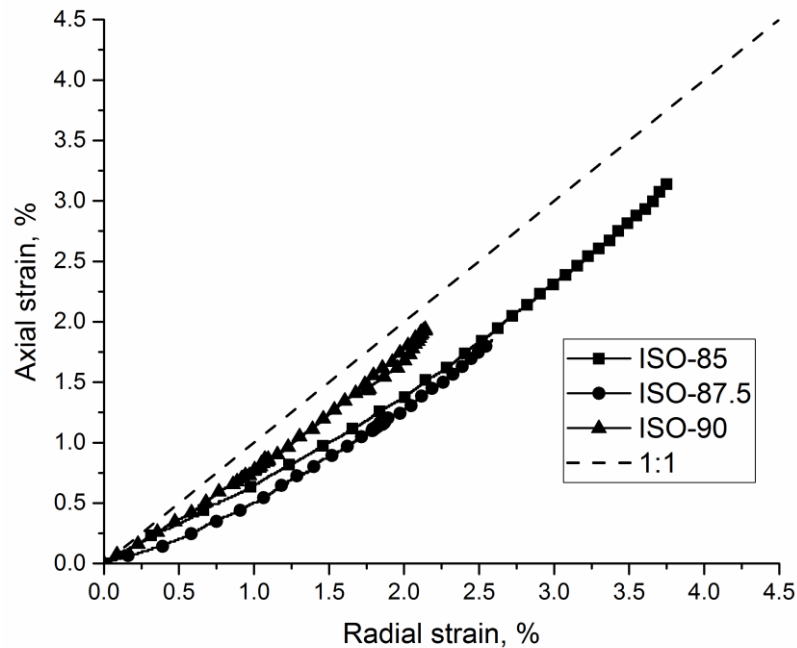


Figure 7. Axial strain versus radial strain during the isotropic compression test

## 5. Shear Behavior and the Critical State

The triaxial compression shearing test was carried out based on the details summarized in Tables 3 and 4 for both the drained and undrained conditions, respectively. Figure 8 indicates the typical stress-strain relation of both the drained and undrained shearing tests. Under the drained conditions, the soil revealed a strain hardening behavior in the low mean effective stress levels 100 and 200 kPa, while a strain softening behavior was present in the higher stress levels 300 and 400 kPa, in which the deviator stress decreased slightly after reaching the peak. Under both the drained and undrained shearing conditions, the soil strength increased significantly as the consolidation stress level increased. Figure 9 indicates the volumetric response during the drained shear, the soil revealed a contractive response, regardless of the mean effective stresses. It is worth to note that the tests were performed on normally consolidated re-compacted specimens, thus the variations of the initial void ratio (i.e., before shearing stage) resulted from different consolidation stresses. The volumetric response under the undrained condition can be indirectly concluded from the stress path shape indicated in Figure 10. For the soil specimens sheared at low consolidated stress level, the soil exhibited firstly contractive response, as the stress path moved to the left direction, and then the soil passed through a phase transformation point at zero dilation, and after that the stress path turned towards the right direction, which is a sign of the tendency to soil dilation. After passing through the phase transformation point, the deviator and mean effective stresses increased with a constant stress ratio until reaching the critical state. The soil specimens sheared at high consolidation stress levels, revealed a slight increase in the mean effective stress at the early stage of shearing. The mean effective stress then decreased significantly after the first phase transformation point. Towards the end of the stress path, the mean effective stress increased again before reaching the critical state and after surpassing the second phase transformation point. Phase transformation points were also observed in the CDG soils reported by Yan and Li [12], Wang and Yan [13] and Lee and Coop [10]. However, no phase transformation revealed for the CDG soil studied by Ng and Chiu [27]. The initial stiffness during the undrained conditions was higher than those in the drained conditions. Nevertheless, the soil exhibited drained strength much more than that in the undrained condition.

The critical state can be reached when the rate of changes in stresses and volume become insignificant. Thus, the critical state of the CDG soil can be estimated by the specimens' state at 30% axial strain, in which there was no significant change in volume and stress as shown in Figures 8 and 9. The critical states have been represented in both the  $q$ - $p'$  and  $e$ - $\log p'$  spaces as depicted in Figures 10 and 11, respectively. The CDG soil showed a unique CSL, irrespective of the drainage conditions and initial states in both the volumetric and stress spaces (i.e.,  $q$ - $p'$  and  $e$ - $\log p'$ ). In the  $q$ - $p'$  space, the CDG soil approached unique CSL at critical stress ratio ( $M$ ) equal 1.5, corresponding to critical friction angle of  $36.8^\circ$ . In the volumetric space  $e$ - $\log p'$ , the CDG soil also revealed a unique CSL parallel to the ICL. Therefore, the state parameter proposed by Been and Jefferies [28]; which is defined as the vertical distance between ICL and CSL in the  $e$ - $\log p'$  space is constant, regardless of mean effective stress levels. The parallelism of the ICL and CSL was also observed in CDG soil studied by Lee and Coop [10]. However, the CDG soils studied by Yan and Li [12] and Ng, Fung [11] showed a non-parallelism of ICL and CSL, where they tended to converge as the effective mean stress increased, which possibly attributed to soils mineralogy and micro-fabric.



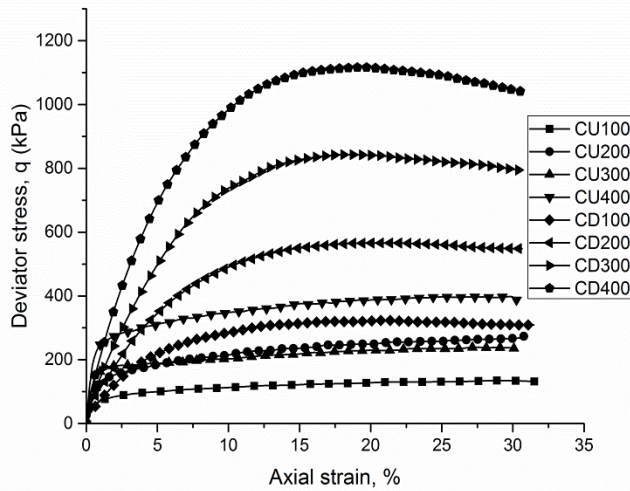


Figure 8. Drained and undrained stress-strain relationship

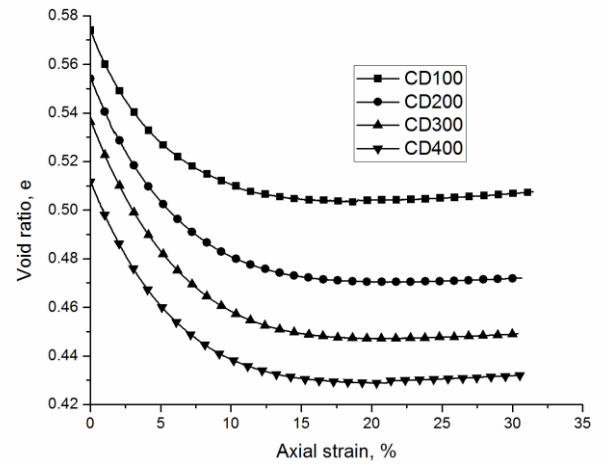


Figure 9. Volumetric response

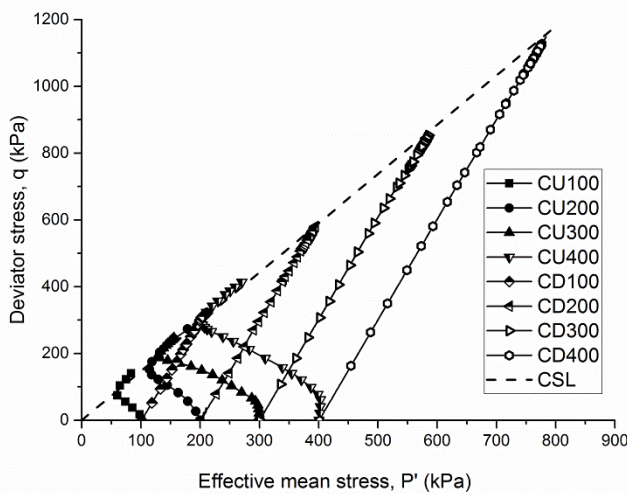


Figure 10. Stress paths of the undrained and drained shearing

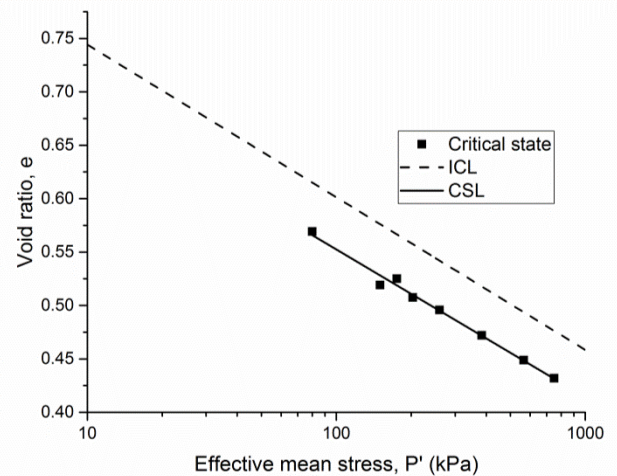


Figure 11. Uniqueness of critical state and isotropic compression lines

## 6. Conclusions

This study presented the results of a set of drained and undrained triaxial shearing and isotropic compression tests on medium-coarse grading CDG soils to investigate their behavior. The experimental results have been interpreted based on the results of the XRD analysis and the scanning electron microscopic-photos. The soil showed low compressible response during the isotropic compression with a unique isotropic compression line. The volumetric change was unrecoverable throughout the unloading path. A 250 kPa effective mean stress was sufficient to erase the induced anisotropy from the moist tamping preparation method, and then the soil showed the isotropic response. After the analysis of the isotropic compression results with the XRD analysis results and the SEM photos, it can be concluded that the soils' mineralogy and micro-fabric are considered paramount factors governing the compression behavior in addition to grading.

The soil exhibited a strain hardening behavior under the undrained conditions, irrespective to the consolidation stress level. Under the drained conditions, the soil revealed a strain hardening at low consolidation stress levels; however, a slight tendency of a strain softening response revealed at high stress levels. The soil exhibited a contractive response under the drained shearing. The undrained response of the soil was complicated, in which the stress path in the low consolidated stress was contractive from the beginning of the shearing and after passing through the phase transformation point, the soil response changed from contractive to dilative, and then both the deviator and mean effective stresses increased with a constant stress ratio until reaching the critical state. In the high consolidation stresses, the soil initially exhibited a dilative response followed by a contractive response, and then a dilative response up to the critical state with two phase transformation points. The soil showed a unique critical state line in both the  $q$ - $p'$  and  $e$ - $\log p'$  spaces, regardless of the drainage conditions and initial states (i.e., void ratio and initial density). The CSL in the  $e$ - $\log p'$  space was parallel to the ICL. The stress ratio at the critical state was 1.5, corresponding to a critical state friction angle of  $36.8^\circ$ .

## 7. Funding

This paper was funded from the National Natural Science Foundation of China (NSFC) (No. 51508216 and 416772267).

## 8. Conflicts of Interest

The authors declare no conflict of interest.

## 9. References

- [1] Ng, C. W. W., P. Guan, and Y. J. Shang. "Weathering Mechanisms and Indices of the Igneous Rocks of Hong Kong." *Quarterly Journal of Engineering Geology and Hydrogeology* 34, no. 2 (May 2001): 133–151. doi:10.1144/qj.2001.34.2.133.
- [2] Rocchi, I., and M. R. Coop. "Mechanisms of Compression in Well-Graded Saprolitic Soils." *Bulletin of Engineering Geology and the Environment* 75, no. 4 (January 2, 2016): 1727–1739. doi:10.1007/s10064-015-0841-7.
- [3] Chiu, C.F., and Charles W.W. Ng. "Relationships Between Chemical Weathering Indices and Physical and Mechanical Properties of Decomposed Granite." *Engineering Geology* 179 (September 2014): 76–89. doi:10.1016/j.enggeo.2014.06.021.
- [4] Irfan, T. Y. "Mineralogy, Fabric Properties and Classification of Weathered Granites in Hong Kong." *Quarterly Journal of Engineering Geology and Hydrogeology* 29, no. 1 (February 1996): 5–35. doi:10.1144/gsl.qj.1996.29.1.02.
- [5] Lumb, Peter. "The Properties of Decomposed Granite." *Géotechnique* 12, no. 3 (September 1962): 226–243. doi:10.1680/geot.1962.12.3.226.
- [6] Vaughan, P., M. Maccarini, and S. Mokhtar, Indexing the engineering properties of residual soil. *Quarterly Journal of Engineering Geology and Hydrogeology*, 1988. 21(1): p. 69-84.
- [7] Rocchi, Irene, M. C. Todisco, and Matthew R. Coop. "Influence of grading and mineralogy on the behaviour of saprolites." In *Proc. 6th Int. Symp. on Deformation Characteristics of Geomaterials*, IS-Buenos Aires, Argentina, pp. 415-422. 2015.
- [8] Ham, Tae-Gew, Yukio Nakata, Rolando P. Orense, and Masayuki Hyodo. "Influence of Gravel on the Compression Characteristics of Decomposed Granite Soil." *Journal of Geotechnical and Geoenvironmental Engineering* 136, no. 11 (November 2010): 1574–1577. doi:10.1061/(asce)gt.1943-5606.0000370.
- [9] Ham, Tae-Gew, Yukio Nakata, Rolando Orense, and Masayuki Hyodo. "Influence of Water on the Compression Behavior of Decomposed Granite Soil." *Journal of Geotechnical and Geoenvironmental Engineering* 136, no. 5 (May 2010): 697–705. doi:10.1061/(asce)gt.1943-5606.0000274.
- [10] Lee, I. K., and M. R. Coop. "The Intrinsic Behaviour of a Decomposed Granite Soil." *Géotechnique* 45, no. 1 (March 1995): 117–130. doi:10.1680/geot.1995.45.1.117.
- [11] Ng, Charles WW, W. T. Fung, C. Y. Cheuk, and Liming Zhang. "Influence of stress ratio and stress path on behavior of loose decomposed granite." *Journal of Geotechnical and Geoenvironmental Engineering* 130, no. 1 (2004): 36-44. doi:10.1061/(ASCE)1090-0241(2004)130:1(36).
- [12] Yan, W.M., and X.S. Li. "Mechanical Response of a Medium-Fine-Grained Decomposed Granite in Hong Kong." *Engineering Geology* 129–130 (March 2012): 1–8. doi:10.1016/j.enggeo.2011.12.013.
- [13] Wang, Y. H., and W. M. Yan. "Laboratory studies of two common saprolitic soils in Hong Kong." *Journal of geotechnical and geoenvironmental engineering* 132, no. 7 (2006): 923-930. doi:10.1061/(ASCE)1090-0241(2006)132:7(923).
- [14] Elkamhawy, Elsayed, Bo Zhou, and Huabin Wang. "Transitional Behavior in Well-Graded Soils: An Example of Completely Decomposed Granite." *Engineering Geology* 253 (April 2019): 240–250. doi:10.1016/j.enggeo.2019.02.027.
- [15] Ietto, Fabio, Francesco Perri, and Federico Cella. "Weathering Characterization for Landslides Modeling in Granitoid Rock Masses of the Capo Vaticano Promontory (Calabria, Italy)." *Landslides* 15, no. 1 (July 13, 2017): 43–62. doi:10.1007/s10346-017-0860-5.
- [16] Elkamhawy, Elsayed, Huabin Wang, Bo Zhou, and Zhiyong Yang. "Failure Mechanism of a Slope with a Thin Soft Band Triggered by Intensive Rainfall." *Environmental Earth Sciences* 77, no. 9 (May 2018). doi:10.1007/s12665-018-7538-8.
- [17] GEO, Geoguide 3—Guide to Rock and Soil Descriptions. Geotechnical Engineering Office, Civil Engineering Department, The Government of the Hong Kong Special Administrative Region. 2017.
- [18] Alavi Nezhad Khalil Abad, S.V., A. Tugrul, C. Gokceoglu, and D. Jahed Armaghani. "Characteristics of Weathering Zones of Granitic Rocks in Malaysia for Geotechnical Engineering Design." *Engineering Geology* 200 (January 2016): 94–103. doi:10.1016/j.enggeo.2015.12.006.

- [19] Ng, Charles WW, and Abraham CF Chiu. "Behavior of a loosely compacted unsaturated volcanic soil." *Journal of Geotechnical and Geoenvironmental Engineering* 127, no. 12 (2001): 1027-1036. doi:10.1061/(ASCE)1090-0241(2001)127:12(1027).
- [20] Zauyah, Siti, Carlos E.G.R. Schaefer, and Felipe N.B. Simas. "Saprolites." *Interpretation of Micromorphological Features of Soils and Regoliths* (2010): 49–68. doi:10.1016/b978-0-444-53156-8.00004-0.
- [21] Skempton, A. W. "The Pore-Pressure Coefficients A and B." *Géotechnique* 4, no. 4 (December 1954): 143–147. doi:10.1680/geot.1954.4.4.143.
- [22] Head, K.H., in *Manual of soil laboratory testing*. 1992, Vol. 3. John Wiley and Sons: New York.
- [23] Verdugo, R. and K. Ishihara, *The steady state of sandy soils*. *Soils and Foundations*, 1996. 36(2): p. 81-91.
- [24] Lee, Jong-Sub, Maria Guimaraes, and J. Carlos Santamarina. "Micaceous sands: Microscale mechanisms and macroscale response." *Journal of Geotechnical and Geoenvironmental Engineering* 133, no. 9 (2007): 1136-1143. doi:10.1061/(ASCE)1090-0241(2007)133:9(1136).
- [25] Zhou, B., and J. Wang. "Random Generation of Natural Sand Assembly Using Micro x-Ray Tomography and Spherical Harmonics." *Géotechnique Letters* 5, no. 1 (January 2015): 6–11. doi:10.1680/geolett.14.00082.
- [26] Ham, Tae-Gew, Yukio Nakata, Rolando Orense, and Masayuki Hyodo. "Strength Anisotropy of Compacted Decomposed Granite Soils." *Geotechnical and Geological Engineering* 30, no. 1 (September 22, 2011): 119–127. doi:10.1007/s10706-011-9454-5.
- [27] Ng, Charles WW, and Abraham CF Chiu. "Laboratory study of loose saturated and unsaturated decomposed granitic soil." *Journal of Geotechnical and Geoenvironmental Engineering* 129, no. 6 (2003): 550-559. doi:10.1061/(ASCE)1090-0241(2003)129:6(550).
- [28] Been, Ken, and Mike G. Jefferies. "A state parameter for sands." *Géotechnique* 35, no. 2 (1985): 99-112.